Shape coexistence in ^{72}Se investigated following the β decay of ^{72}Br

E. A. McCutchan, C. J. Lister, T. Ahn, R. J. Casperson, A. Heinz, G. Ilie, J. Qian, E. Williams, R. Winkler, and V. Werner

Phys. Rev. C **83**, 024310 — Published 18 February 2011

DOI: 10.1103/PhysRevC.83.024310

Shape coexistence in ^{72}Se investigated following the β-decay of ^{72}Br

E.A. McCutchan[1], C.J. Lister[1], T. Ahn[2], R.J. Casperson[2], A. Heinz[2], G. Ilie[2,3], J. Qian[2], E. Williams[2], R. Winkler[2], and V. Werner[2]
[1] *Physics Division, Argonne National Laboratory, Argonne, Illinois 60439, USA*
[2] *Wright Nuclear Structure Laboratory, Yale University, New Haven, CT 06520 USA and*
[3] *National Institute for Physics and Nuclear Engineering, P.O. Box MG-6, Bucharest, Romania*

The structure of ^{72}Se was investigated following the ϵ/β^+-decay of ^{72}Br produced in the ^{58}Ni(^{16}O, pn) reaction at 50 MeV. Using a beam chopping system, off-beam γ-ray decay data was collected with an array of Clover Ge detectors. γ-γ coincidence measurements provided a significant modification of the prior level scheme and γ-γ angular correlation measurements allowed spin determinations and multipole mixing ratio extraction. The new information on the non-yrast states were combined with previous in-beam data to investigate the issue of shape coexistence by comparing to various configuration mixing approaches. Clear evidence for shape coexistence is found, with a ground state of modest, or slightly oblate, deformation and a well-deformed prolate shape which would lie at an unperturbed excitation of 875 keV. The shape mixing is near complete at low spin.

I. INTRODUCTION

Shape coexistence in the light Selenium isotopes has been the subject of intense debate in the last few years, with evidence presented for oblate ground states [1, 2], which was challenged [3], supported [4], and once more cast in doubt [5]. Independent of the interpretation of the ground state structure, the dynamic behavior becomes dominated by prolate collective rotation, at modest ($\sim$1 MeV) excitation energy. In fact, shape coexistence in the Selenium isotopes has a long history, and ^{72}Se was one of the first nuclei ever found to show such behavior [6–8]. The topic remains important today as shape coexistence and mixing in these nuclei continues to be a theoretical challenge and a real testing ground for shell-model and density functional approaches. New interest and measurements in Se have fostered a number of microscopic calculations [3, 4, 9–11]. However, to complement these approaches, more empirical methods quantifying the configuration mixing are still important analysis tools. The key issues which need inferring are the exact competing shapes, their relative excitation, and the degree of mixing between shapes. The most controversial aspect is experimentally differentiating between soft-spherical shapes which vibrate, and true oblate shapes with small deformation that are rotating collectively.

The most defining experimental signature of shape coexistence in this region is the presence of a low-lying (<1 MeV) $J^\pi = 0^+$ state, with a configuration significantly different from the ground state structure. This is the case in ^{72}Se, where the first excited 0^+ state lies only 75 keV above the 2_1^+ state. Furthermore, the moment of inertia of the ground state band exhibits pronounced irregularities. Figure 1 illustrates these unusual features with a plot of $2I/\hbar^2$ versus $(\hbar\omega)^2$ for the ground state bands of ^{68,70,72,74}Se. ^{68}Se has a smoothly evolving band interpreted [1] as collective oblate rotation. In ^{70,72}Se, the low-spin states are significantly perturbed, while the states with $J > 6$ follow the behavior expected for a rotational band with constant moment of inertia and constant deformation. For ^{74}Se, the moment of inertia evolves more smoothly than in ^{70,72}Se, however, there are still some obvious departures from that expected for a regular rotational band.

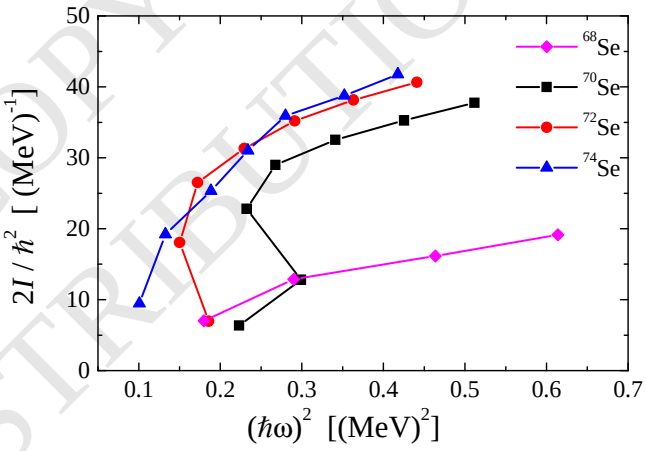

FIG. 1: (Color online) Plot of $2I/\hbar^2$ versus $(\hbar\omega)^2$ for the yrast bands of ^{68,70,72,74}Se.

Ref. [6] first observed the irregularities in the moment of inertia of the ground state band of ^{72}Se and that the energies and decay properties of the low-lying states did not agree with the simple model of a spherical vibrational nucleus. Based on these observations, the excited 0^+ state and states of the yrast band with $J > 4$ were interpreted [6–8] as a deformed K^π=0^+ band coexisting with vibrational states coming from a spherical ground state. The first 2^+ states in ^{72}Se were discussed in terms of strong mixtures of 1-phonon vibrational and rotational states. Later, Lieb and Kolata [12] analyzed ^{72}Se in a variety of different models, including the rotational and vibrational limits of the geometric collective model, simple two-level mixing, as well as the interacting boson model (IBM). Their conclusion was that all known observables in ^{72}Se could not be adequately described by any of the simple models.

More recently, lifetimes in the yrast band of ^{72}Se have

been remeasured [4] with high precision. In the same work, Hartee-Fock-Bogoliubov (HFB)-based configuration mixing calculations predicted oblate character for the 2_1^+ state, evolving into a prolate shape for the 4^+ and 6^+ members of the ground state band. Subsequent microscopic calculations [9] of the light Se isotopes using the adiabatic time-dependent HFB method provide a similar picture. In these calculations, the 0_1^+ state is oblate in character, the 2_1^+ state is a complete mixture of oblate and prolate shapes, while the 4_1^+ and 6_1^+ states show increasingly prolate wave functions.

The underlying microscopic driver for this shape coexistence lies in the single particle states in the N,Z = 28-50 shell, with negative parity fp orbits low in the shell and the intruder $1g_{9/2}$ orbit higher. States with dominant fp occupancy tend to show softness, or small oblate deformation, while states with significant $1g_{9/2}$ occupancy are highly deformed. All Nilsson-like calculations show similar features, with significant gaps between Nilsson orbitals both for oblate and prolate deformation at N,Z = 34 to 38. However, the size of the gaps and their dependence on deformation, β, and triaxiality, γ, differ from model to model. These differences lead to significantly different predicted shape landscapes with different binding energy minima and different barriers between them. Experimental data should be able to differentiate between these models. However, to unfold the coexistence, especially to delineate the substantial mixing due to low separation barriers, requires rather complete spectroscopy. This paper is aimed at improving the data on relatively low-spin non-yrast states in ^{72}Se.

Several studies have investigated ^{72}Se in beam, so the purpose of this project was to provide new complimentary data from β-decay. It builds on the pioneering decay work of Collins *et al.,* [8]. ^{72}Br has two β-decaying states with J = 1,3, so it populates a wide variety of low-spin states. The large Q value of 8799(7) keV allows states above 4 MeV to be observed. The use of a modern array of Compton suppressed detectors at many angles provided very high quality data. These data allowed new states to be seen, some errors to be identified and numerous branching ratio and angular correlation measurements which are critical to the question of shape mixing.

II. EXPERIMENT

Excited states in ^{72}Se were populated in the ϵ/β^+ decay of ^{72}Br and studied through off-beam, γ-ray spectroscopy. The parent ^{72}Br nuclei were produced in the ^{58}Ni(^{16}O, pn) reaction. The ∼10 pnA, 50 MeV ^{16}O beam was provided by the ESTU tandem accelerator at the Wright Nuclear Structure Laboratory at Yale University. The target consisted of 5.9-mg/cm^2 ^{58}Ni which was of sufficient thickness to stop all recoiling nuclei. There have been lengthy controversies over the spin/parity assignments for the β-decaying states in ^{72}Br. The data

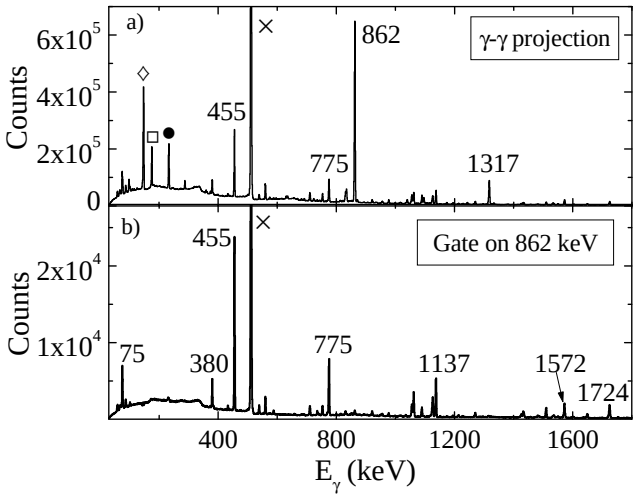

FIG. 2: (a) Projection of the delayed γ-γ coincidence matrix. Intense transitions belong to ^{72}Se are indicated by their energy in keV. Contaminant transitions are labeled by the symbols (• ^{69}Ge), (□ ^{71}Ge), (◇ ^{71}As), and (× 511 keV annihilation). (b) Spectrum gated on the 862-keV, $2_1^+ \rightarrow 0_1^+$ transition in ^{72}Se.

have been collected and issues resolved in the most recent A = 72 compilation [13]. The parent ^{72}Br has a ground state of spin and parity $J^\pi = 1^+$ with $T_{1/2}$ = 78.6 sec and a β-decaying isomeric state with spin and parity $J^\pi = 3^-$ and $T_{1/2}$ = 10.6 sec. The experiment was performed with a beam-on/beam-off cycle of 30 sec. With the present setup, it was not possible to distinguish between the ground state and isomeric decays.

In the beam-off cycle, γ rays were detected with ten Compton-suppressed segmented YRAST Ball Clover HPGe detectors. The detectors were located 21.5 cm from the target position. The array photopeak efficiency was ∼1% at 1.3 MeV and covered an energy range from ∼50 keV to 4000 keV. Both γ-ray singles and γ-γ coincidence data were collected in event mode. Six hours of data were collected with a singles trigger and thirty four hours of data were collected with a doubles trigger, yielding 4.0×10^7 Clover singles events and 5.4×10^7 Clover-Clover coincidence pairs, respectively.

Energy and efficiency calibrations were performed using standard sources of ^{133}Ba, ^{152}Eu, and ^{226}Ra. Data were sorted in histograms and matrices using the CSCAN sorting package [14]. The analysis was performed using the Radware package [15]. The projection of the γ-γ coincidence matrix is shown in Fig. 2(a). ^{72}Se is the strongest observed channel. Significant contaminant channels include ^{69,71}Ge and ^{71}As. The quality of the coincidence data is illustrated in Fig. 2(b) with a gate on the 862-keV, $2_1^+ \rightarrow 0_1^+$ transition, showing only γ rays from ^{72}Se.

γ-γ coincidence measurements were used to construct the level scheme and, in most cases, measure transition intensities. In addition, select angular correlation measurements were performed for strongly populated cascades. For these measurements, the Clover detectors

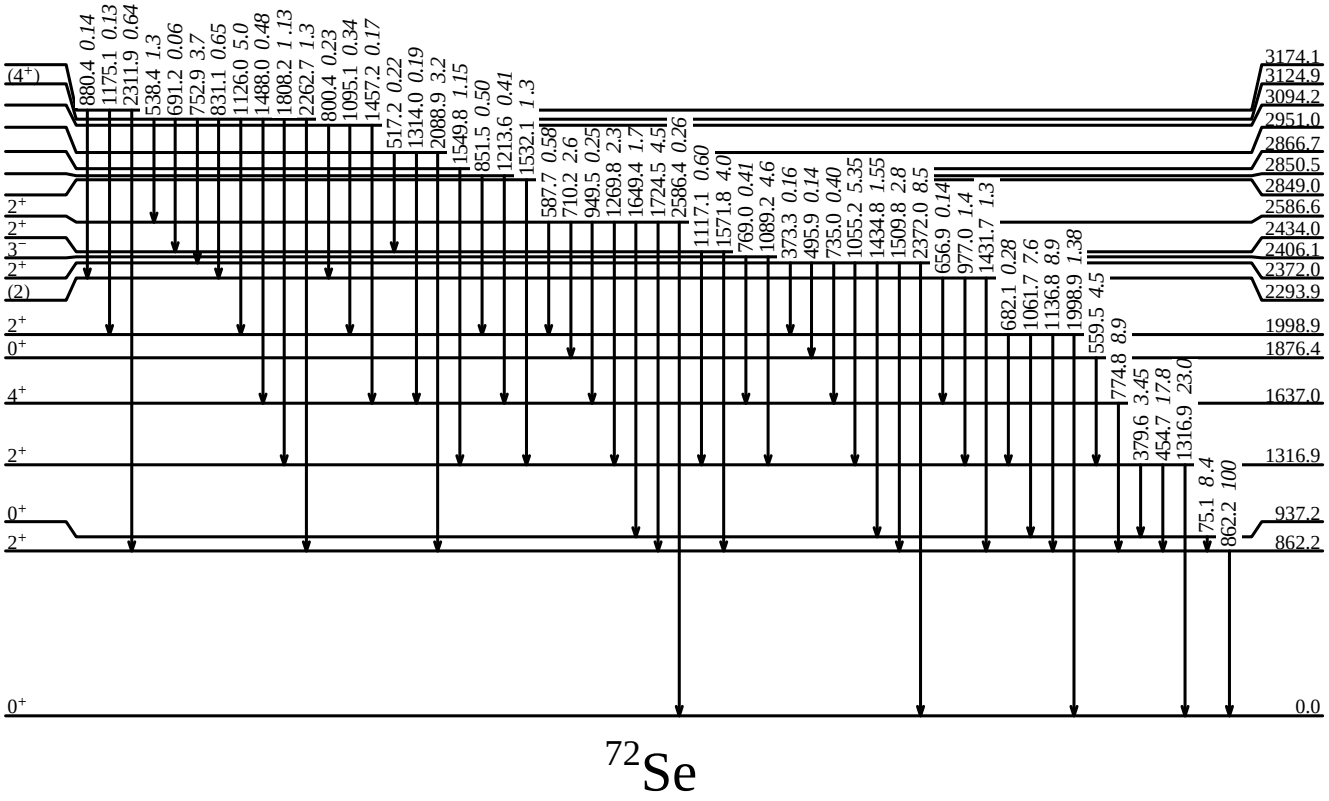

FIG. 3: Level scheme of ^{72}Se populated in the $\epsilon/beta^+$ decay of ^{72}Br for levels below 3200 keV. Levels and transitions are labeled by their energy in keV. γ-ray transitions are also labeled by their relative intensity (in italics), normalized to the 862-keV, $2_1^+ \rightarrow 0_1^+$ transition ($I_{862} \equiv 100$). The energies and decay properties of additional new levels above 3200 keV are summarized in Table 1.

were positioned at relative, first quadrant angles of 20.0°, 40.1°, 49.3°, 55.5°, 59.5°, 64.8°, 70.5°, and 82.2°.

The level scheme obtained in the present work provides a substantial modification to the literature ϵ/β^+ decay data [13] on ^{72}Se. The evaluated data originates mainly from Ref. [8], which used an identical reaction as in the present work to produce the parent ^{72}Br nuclei. The only other prior experimental study on the decay of ^{72}Br is from Refs. [6, 7], which measured the lifetime and decay properties of the 0_2^+ state at 937 keV. In the present work, no evidence is found for four levels previously proposed in β decay, twenty five new levels are identified, and the decay properties of several levels are significantly modified. Table I summarizes the levels populated in ^{72}Se and their γ-decay. The present level scheme for levels populated below 3200 keV is given in Fig. 3.

A. Discussion of Levels

The 0_2^+ level at 937 keV has been well established in several experiments [13]. Two independent measurements for the lifetime of the level yielded values of $\tau =$ 22.9(14) ns [6] and $\tau = 27.8(6)$ ns [16]. The ratio of $E0$ to $E2$ decays was determined in Refs. [6, 7] to be 0.37(23). This measurement was performed by comparing the intensities of the 1137-keV transition (which directly feeds the 2_1^+ state) and the 1062-keV transition (which directly feeds the 0_2^+ state) in the singles and coincidence spectra. In the present work, we perform a similar analysis, however, since the singles spectrum is quite complicated and the chance for overlapping contaminent peaks large, the ratio is extracted using gates from above and below the 0_2^+ state. In a gate on the 1126-keV transition, the relative intensities of the 1137-keV and 1062-keV transitions are determined. These are compared to the intensities obtained by gating from below on the 862-keV, $2_1^+ \rightarrow 0_1^+$ transition. From the difference in intensities obtained for the 1062-keV transition, the $E0/E2$ ratio is determined as 0.41(8), consistent with the previous measurement but providing a signficant reduction in error. The $B(E2;0_2^+ \rightarrow 2_1^+)$ strength calculated with the new $E0/E2$ ratio is 159(20) W.u.

A 2^+ level at 1317 keV has been identified in both β decay and (HI,xn) reactions [13] and observed to decay to the 0_2^+, 2_1^+ and 0_1^+ states through transitions of 380, 455, and 1317 keV, respectively. In the present work, the 455-keV and 1317-keV branches are confirmed and found to have intensities consistent with the literature values. The intensity of the 380-keV transition was reported [13] as about half that of the 455-keV transition.

TABLE I: Levels populated in ^{72}Se and their γ decay. Relative intensities (in β decay) for γ-ray transitions depopulating the levels are given. I_γ gives the intensity in β decay normalized to $2_1^+ \rightarrow 0_1^+ \equiv 100$, while B_γ gives the relative intensity from each level, normalized to the strongest branch. Relative intensities from each of the levels are also compared with literature values, B_{lit} [13], where available.

$J_i^{\pi\,a}$	E_i (keV)	J_f^π	E_f (keV)	E_γ (keV)	I_γ	B_γ	B_{lit}^b
2^+	862.18(7)	0^+	0.00	862.18(7)	100(4)	100(4)	100
0^+	937.24(20)	2^+	862.18	75.06(20)	8.4(14)	100(17)	100
2^+	1316.91(8)	0^+	0.00	1316.90(8)	23.0(12)	100(5)	100(6)
		2^+	862.18	454.74(7)	17.8(9)	77(4)	76(5)
		0^+	937.24	379.56(8)	3.45(17)	15(1)	35(2)
4^+	1636.98(8)	2^+	862.18	774.80(8)	8.9(5)	100(6)	100
$0^{+\,c}$	1876.39(9)	2^+	1316.91	559.48(8)	4.5(3)	100(7)	100(6)
		2^+	862.18	1014.2^d	<0.05	<1	27(14)
2^+	1998.92(9)	0^+	0.00	1998.91(10)^e	1.38(14)	16(2)	
		2^+	862.18	1136.76(8)	8.9(4)	100(5)	100(10)
		0^+	937.24	1061.67(9)	7.6(5)	85(6)	79(7)
		2^+	1316.91	682.1(2)^e	0.28(4)	3.2(5)	
(2)	2293.90(10)^f	2^+	862.18	1431.74(10)	1.3(2)	93(14)	87(3)
		2^+	1316.91	976.98(9)	1.4(1)	100(7)	100(8)
		4^+	1636.98	656.9(2)^e	0.14(3)	10(2)	
$2^{+\,c}$	2372.03(9)	0^+	0.00	2372.01(10)	8.5(6)	100(6)	100(10)
		2^+	862.18	1509.84(9)	2.8(2)	33(2)	44(7)
		0^+	937.24	1434.75(9)	1.55(16)	18(2)	13(5)
		2^+	1316.91	1055.17(8)	5.35(35)	63(4)	50(8)
		4^+	1636.98	735.03(9)^e	0.40(4)	4.7(5)	
		0^+	1876.39	495.9(3)^e	0.14(2)	1.6(2)	
		2^+	1998.92	373.3(3)^e	0.16(3)	1.9(4)	
3^-	2406.05(10)^f	2^+	1316.91	1089.18(9)	4.6(4)	100(9)	100
		4^+	1636.98	769.03(15)^e	0.41(6)	8.9(13)	
$2^{+\,c}$	2433.98(10)	0^+	0.00	2434.0^d	<0.1	<2.5	33(7)
		2^+	862.18	1571.78(10)	4.0(3)	100(8)	100(5)
		2^+	1316.91	1117.12(14)	0.60(5)	15(1)	25.0(19)
$2^{+\,g}$	2586.63(10)	0^+	0.00	2586.4(3)^e	0.26(3)	5.8(7)	
		2^+	862.18	1724.46(9)	4.5(3)	100(7)	100(8)
		0^+	937.24	1649.41(15)^e	1.7(2)	38(4)	
		2^+	1316.91	1269.82(12)	2.3(2)	51(4)	24(12)
		4^+	1636.98	949.5(2)^e	0.25(3)	5.6(7)	
		0^+	1876.39	710.18(9)	2.6(2)	58(4)	47(10)
		2^+	1998.92	587.7(2)^e	0.58(6)	13(1)	
	2849.0(2)^h	2^+	1316.91	1532.1(2)^e	1.3(2)	100(15)	
	2850.5(2)^h	4^+	1636.98	1213.6(2)^e	0.41(8)	82(16)	
		2^+	1998.92	851.5(2)^e	0.50(15)	100(30)	
	2866.7(1)^h	2^+	1316.91	1549.8(1)^e	1.15(18)	100(16)	
	2951.11(15)^h	2^+	862.18	2088.9(2)^e	3.2(3)	100(9)	
		4^+	1636.98	1314.05(15)^e	0.19(4)	5.9(12)	
		2^+	2433.98	517.2(2)^e	0.22(4)	6.9(13)	
	3094.17(11)^h	4^+	1636.98	1457.2(2)^e	0.17(3)	50(9)	
		2^+	1998.92	1095.10(15)^e	0.34(5)	100(15)	
		(2)	2293.90	800.4(2)^e	0.23(3)	68(9)	

TABLE I: (continued)

$J_i^{\pi a}$	E_i (keV)	J_f^{π}	E_f (keV)	E_γ (keV)	I_γ	B_γ	B_{lit}
(4^+)	3124.93(10)	2^+	862.18	2262.7(2)^e	1.3(1)	26(2)	
		2^+	1316.91	1808.21(10)	1.13(12)	23(2)	33(7)
		4^+	1636.98	1488.0(2)^e	0.48(7)	9.6(14)	
		2^+	1998.92	1125.96(9)	5.0(4)	100(8)	100(11)
		(2)	2293.9	831.1(2)^e	0.65(7)	13(1)	
		2^+	2372.03	752.88(9)	3.7(3)	74(6)	55(8)
		2^+	2433.98	691.2(3)^e	0.06(3)	1.2(6)	
		2^+	2586.63	538.36(10)	1.3(1)	26(2)	24(8)
	3174.14(20)^h	2^+	862.18	2311.92(15)^e	0.64(8)	100(13)	
		2^+	1998.92	1175.1(2)^e	0.13(3)	20(5)	
		(2)	2293.90	880.4(2)^e	0.14(3)	22(5)	
	3294.67(9)^h	2^+	862.18	2432.50(10)^e	2.3(2)	100(9)	
		2^+	1316.91	1977.78(12)^e	1.12(9)	49(4)	
		2^+	1998.92	1295.7(2)^e	0.18(4)	7.8(17)	
	3327.07(10)^h	2^+	862.18	2465.2(3)^e	1.8(3)	100(17)	
		2^+	1316.91	2010.4(3)^e	0.45(7)	25(4)	
		4^+	1636.98	1690.0(3)^e	0.12(2)	6.7(11)	
		2^+	1998.92	1328.2(2)^e	0.25(4)	14(2)	
		(2)	2372.03	955.02(9)^e	0.98(10)	54(6)	
		3^-	2406.05	920.93(9)^e	1.4(2)	78(11)	
		2^+	2433.98	893.2(2)^e	0.14(3)	7.8(17)	
		2^+	2586.63	740.5(2)^e	0.22(3)	12(2)	
(1,2)	3424.14(12)^h	0^+	0.00	3424.0(2)^e	0.3(1)	26(9)	
		2^+	1316.91	2107.3(2)^e	0.91(8)	80(7)	
		0^+	1876.39	1548.2(3)^e	0.12(3)	11(3)	
		2^+	1998.92	1425.10(10)^e	1.14(9)	100(8)	
		2^+	2372.03	1052.2(2)^e	0.3(1)	26(9)	
		3^-	2406.05	1018.0(2)^e	0.27(4)	24(4)	
	3469.2(2)^h	0^+	0.00	3469.1(2)^e	0.2(1)	9(5)	
		2^+	862.18	2607.1(2)^e	2.3(3)	100(13)	
		2^+	2433.98	1035.2(2)^e	0.31(5)	13(2)	
(1,2)	3480.65(15)^h	0^+	0.0	3480.5(2)^e	0.4(2)	33(17)	
		2^+	862.18	2618.6(3)^e	1.2(2)	100(17)	
		0^+	1876.39	1604.2(2)^e	0.52(10)	43(8)	
		2^+	1998.92	1481.7(1)^e	0.75(11)	62(9)	
		2^+	2372.03	1108.6(2)^e	0.39(7)	32(6)	
(2,3,4)	3557.63(15)^h	2^+	862.18	2695.5(2)^e	0.40(8)	33(7)	
		4^+	1636.98	1920.6(2)^e	0.39(7)	32(6)	
		2^+	1998.92	1558.8(2)^e	0.23(6)	19(5)	
		2^+	2433.98	1123.72(12)^e	1.2(2)	100(17)	
		(4^+)	3124.93	432.65(9)^e	0.58(7)	48(6)	
			3327.07	230.5(2)^e	0.31(6)	26(5)	
	3584.8(2)^h	2^+	862.18	2722.6(2)^e	1.3(2)	100(15)	
(2,3,4)	3600.12(12)^h	2^+	862.18	2738.2(2)^e	1.6(3)	88(16)	
		2^+	1316.91	2283.25(15)^e	1.8(2)	100(11)	
		4^+	1636.98	1963.2(2)^e	0.74(9)	41(5)	
		2^+	2372.03	1228.2(1)^e	0.72(8)	40(4)	
		3^-	2406.05	1194.0(1)^e	0.73(9)	40(5)	
		2^+	2586.63	1013.6(2)^e	0.30(6)	16(3)	

TABLE I: (continued)

$J_i^{\pi\,a}$	E_i (keV)	J_f^π	E_f (keV)	E_γ (keV)	I_γ	B_γ	B_{lit}
	3717.2(2)[h]	0^+	0.00	3717.1(3)[e]	0.23(11)	32(15)	
		2^+	862.18	2855.0(2)[e]	0.71(11)	100(15)	
		2^+	1316.91	2400.2(2)[e]	0.23(5)	32(7)	
	3830.11(15)[h]	2^+	862.18	2968.0(2)[e]	0.40(7)	49(9)	
		2^+	1316.91	2513.3(1)[e]	0.82(8)	100(10)	
		4^+	1636.98	2193.1(2)[e]	0.31(5)	38(6)	
		2^+	1998.92	1831.2(2)[e]	0.22(3)	27(4)	
		(2)	2293.90	1536.2(2)[e]	0.34(4)	41(5)	
		2^+	2372.03	1458.0(3)[e]	0.18(5)	22(6)	
		2^+	2433.98	1396.3(3)[e]	0.14(3)	17(4)	
	3909.3(2)[h]	2^+	862.18	3047.8(3)[e]	0.83(17)	75(17)	
		2^+	1316.91	2592.5(2)[e]	0.98(13)	100(13)	
		2^+	1998.92	1910.1(2)[e]	0.72(10)	73(10)	
		(2)	2293.90	1615.2(2)[e]	0.82(15)	84(15)	
		2^+	2372.03	1537.14(3)[e]	0.12(2)	12(2)	
		2^+	2433.98	1475.2(2)[e]	0.19(4)	19(4)	
		2^+	2586.63	1322.8(2)[e]	0.39(8)	40(8)	
			3294.67	614.7(3)[e]	0.10(5)	10(5)	
	3933.7(2)[h]	2^+	862.18	3071.5(2)[e]	0.53(9)	100(17)	
	3969.8(2)[h]	2^+	1316.91	2652.9(2)[e]	0.75(8)	71(8)	
		4^+	1636.98	2332.9(2)[e]	1.05(15)	100(14)	
	4055.0(2)[h]	4^+	1636.98	2418.0(2)[e]	0.24(4)	100(17)	
	4065.2(2)[h]	2^+	1316.91	2748.3(2)[e]	0.68(8)	100(12)	
	4073.0(4)[h]	2^+	1316.91	2756.6(3)[e]	0.84(8)	59(6)	
		2^+	1998.92	2073.6(4)[e]	1.7(2)	100(12)	
		2^+	2433.98	1638.4(4)[e]	0.14(3)	8.2(17)	
	4080.2(4)[h]	2^+	1316.91	2763.5(3)[e]	0.78(9)	100(10)	
		2^+	2433.98	1645.7(2)[e]	0.09(3)	12(4)	
	4094.8(4)[h]	2^+	1316.91	2778.2(3)[e]	1.00(9)	100(9)	
		4^+	1636.98	2457.6(3)[e]	0.41(6)	41(6)	
		(2)	2293.90	1800.9(2)[e]	0.20(3)	20(3)	
	4188.1(3)[h]	2^+	1998.92	2188.9(3)[e]	0.22(5)	49(11)	
		2^+	2433.98	1754.2(3)[e]	0.27(5)	60(11)	
		2^+	2586.63	1601.5(2)[e]	0.45(6)	100(13)	
	4246.1(3)[h]	2^+	1316.91	2929.5(3)[e]	0.27(5)	82(15)	
		2^+	1998.92	2246.9(3)[e]	0.33(6)	100(18)	
		(2)	2293.9	1952.2(4)[e]	0.074(30)	22(9)	

[a] Level spin assignments are nominal assignments from the evaluation [13], except as noted.
[b] Literature values for branches are from the evaluated data [13].
[c] New spin assignment for previously observed level is given on the basis of angular correlation measurements.
[d] Previously observed transition, unobserved in present work.
[e] New γ-ray transition.
[f] Level was previously observed but not in β decay.
[g] New spin assignment for previously observed level is given on the basis of observed transitions to levels of known spin.
[h] Newly observed level.

Since the efficiency for detecting the low-energy 75-keV, $0_2^+ \rightarrow 2_1^+$ transition was not precisely known, the intensity of the 380-keV transition was determined relative to the other depopulating transitions using gates on transitions feeding the 2_2^+ level. Figure 4(a) illustrates the relative intensities of the transitions depopulating the 1317-keV level using a gate on the 1089-keV feeding transition. From a number of gates on strong transitions feeding the

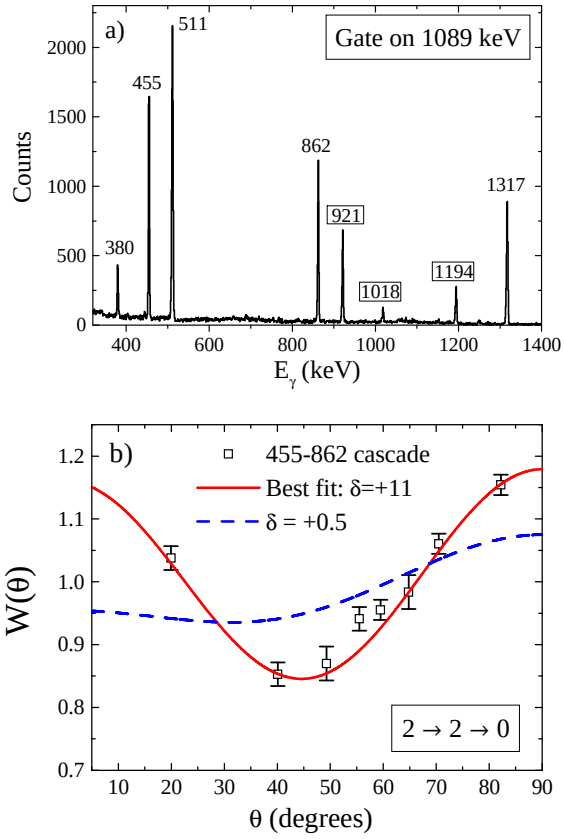

FIG. 4: (Color online) (a) Spectrum gated on the 1089-keV transition which originates from a level at 2406 keV and populates the level at 1317 keV. The peaks in boxes indicate new transitions feeding the level at 2406 keV. (b) Angular correlation analysis for the 455-862 keV, $2 \rightarrow 2 \rightarrow 0$ cascade. The solid line shows the best fit with $\delta = +11$, and for comparison, the dotted line shows the theoretical curve for $\delta = +0.5$.

1317-keV level, the intensity of the 380-keV transition is found to be about a factor of five smaller than that of the 455-keV transition (see Table I). The change in intensity of the 380-keV transition has a significant effect on the $B(E2;\ 2_2^+ \rightarrow 0_2^+)$ strength. Using the measured lifetime of τ=12.6(4) ps [13] and the new intensity for the 380-keV transition, yields $B(E2;\ 2_2^+ \rightarrow 0_2^+) = 36(3)$ W.u.

Angular correlation measurements confirmed the 2^+ spin assignment for this level. The $E2/M1$ character of the 455-keV, $2_2^+ \rightarrow 2_1^+$ transition was determined by gating on the 862-keV transition and determining the intensity of the 455-keV transition in each of the different angle groups. Data from the angular correlation analysis are given in Fig. 4(b) and compared with the best fit δ, as well as with a δ value corresponding to a mixed $E2/M1$ transition. These results show that the 455-keV, $2_2^+ \rightarrow 2_1^+$ transition is nearly pure $E2$, with a measured δ of $+11^{+11}_{-4}$. Combining the newly measured δ with the lifetime of the level and the intensity branch gives $B(E2;\ 2_2^+ \rightarrow 2_1^+) = 75(5)$ W.u.

A level at 1876 keV was previously proposed [8] to decay to the 2_1^+ and 2_2^+ levels through transitions of 1014 keV and 559 keV, respectively, and was tentatively assigned possible spin values of (2,4). In the present work, the 559-keV transition to the 2_2^+ state was confirmed. A 1014-keV transition was observed in coincidence with known lines in ^{72}Se, however, the γ-γ data yielded a different placement in the level scheme. In a gate on the 710-keV transition, which feeds the 1876 keV-level, a strong coincidence is observed with the 559-keV transition and only a very weak coincidence with a 1014-keV transition, as shown in Fig. 5(a). The previous branches for the 559-keV and 1014-keV transitions were reported [8] as approximately 4 to 1, respectively, which is clearly not observed in the 710-keV gate. In a gate on the 1014-keV transition, coincidences are observed with both the 559-keV and 710-keV transitions as well as with a 1724-keV transition, as shown in Fig. 5(b). Both the 710-keV and 1724-keV transitions depopulate a level at 2587 keV and thus the 1014-keV transition is given an alternate placement as direcly populating the 2587-keV level.

The level at 1876 keV is now supported by a single depopulating transition to the 2_2^+ state at 1317 keV. In the γ-γ angle matrices gated on the 1317-keV, $2_2^+ \rightarrow 0_1^+$ transition, most transitions show small variations between the different angle groups, whereas the intensity of the 559-keV transition is significantly enhanced in the 20° angle group, as shown in Fig. 6. This is indicative of a $0 \rightarrow 2 \rightarrow 0$ cascade. Full analysis of the angular correlation data (inset of Fig. 6) supports a spin assignment of 0^+ for the level at 1876 keV. This newly identified 0^+ state fits into the systematics of the neighboring Se isotopes. A high-lying 0^+ state is observed at similar energies in both ^{70}Se [$E(0^+) = 2011$ keV] and ^{74}Se [$E(0^+) = 1657$ keV]. The $E0/E2$ decay ratio is determined from an analysis similiar to that used for the 0_2^+ level. The intensities of the 710-keV and 1270-keV transitions were determined by gating from above on the 538-keV transition and gating from below on the 455-keV transition. The same intensity, within errors, for the 710-keV transition was obtained in both gates, indicating a very small, if any, $E0$ decay for the 1876-keV level.

A 2^+ level at 1999 keV has been reported [13] on the basis of two depopulating transitions of 1062 keV and 1137 keV to the 0_2^+ and 2_1^+ states, respectively. These transitions were confirmed and found to have intensity branches consistent with the literature values. Two new depopulating transitions of 682 keV and 1999 keV to the 2_2^+ and 0_1^+ states, respectively, were identified from the present coincidence data. Gating on the 1125-keV transition, which strongly populates the 1999-keV level, coincidences are observed with the previously identified depopulating transitions of 1062 keV and 1137 keV, as well as the newly identified transitions of 682 keV and 1999 keV, as shown in Fig. 7. Angular correlation analysis of the 1137-862 keV cascade confirmed the 2^+ spin assignment for this level. In addition, the 1137-keV transition is found to be mainly $E2$ in character, with a measured

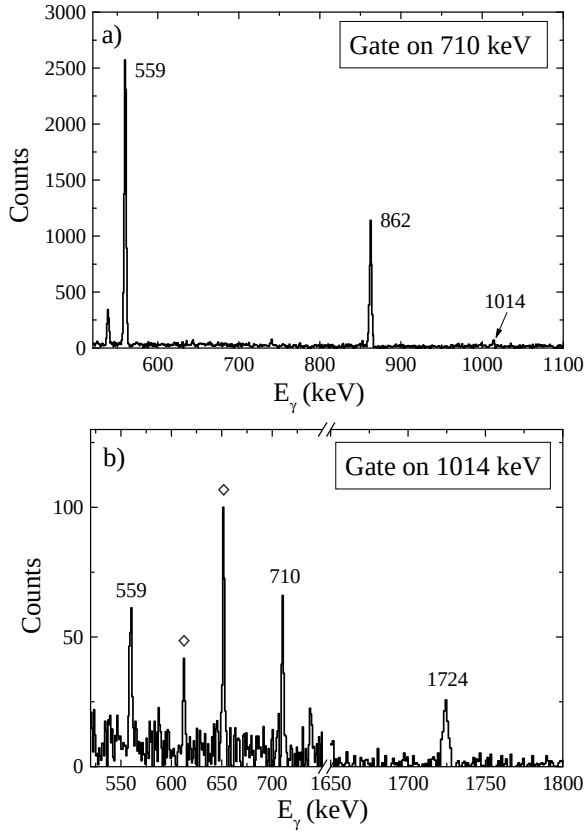

FIG. 5: Spectra providing support for the new placement of a 1014-keV transition in ^{72}Se. (a) Spectrum gated on the 710-keV transition which feeds the level at 1876 keV showing the strong depopulating transition of 559 keV and a very weak coincidence with a 1014-keV transition. (b) Spectrum gated on the 1014-keV transition illustrating coincidences with 710-keV and 1724-keV transitions, both of which depopulate a level at 2587 keV. The ◇ indicates lines coincident with an overlapping 1016-keV transition in ^{68}Ge.

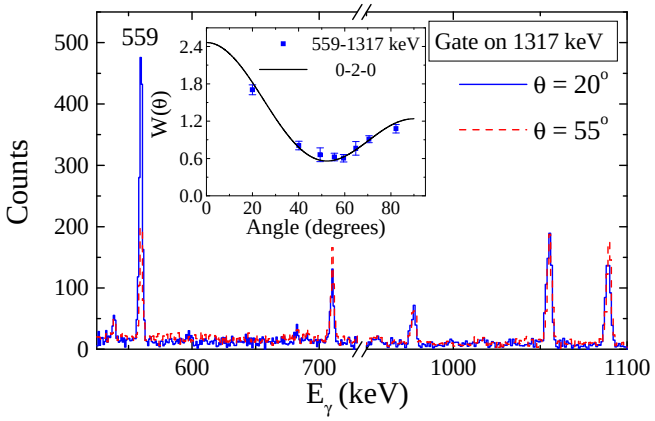

FIG. 6: (Color online) Spectra gated on the 1317-keV transition showing the region between 500-1100 keV for detectors at relative angles of 20° (blue solid line) and 55° (red dashed line). The two spectra are normalized such that the 1055-keV transition has equal intensities for both spectra. The inset gives the angular correlation analysis for the 559-1317 keV cascade in ^{72}Se.

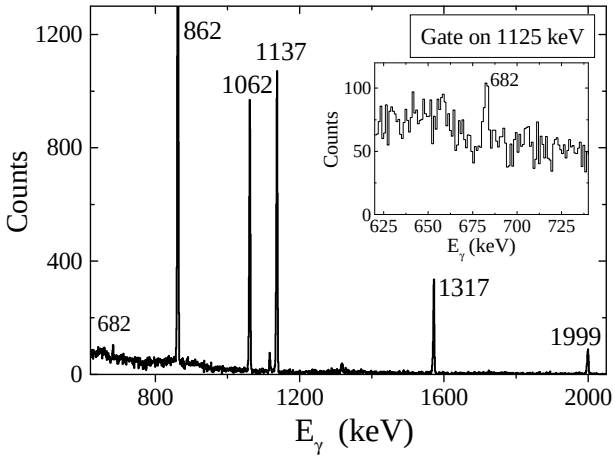

FIG. 7: Spectrum obtained by gating on the 1125-keV transition which feeds the level at 1999 keV. Previously identified depopulating transitions of 1062 keV and 1137 keV are observed as well as newly identified depopulating transitions of 682 keV and 1999 keV. The inset gives the spectrum expanded in the energy region around the 682 keV-transition.

δ of -8^{+3}_{-12}.

A level at 2150 keV was previously proposed [8] in β decay on the basis of three depopulating transitions; a 2151-keV transition to the ground state, a 832-keV transition to the 2^+_2 state and a tentative 512-keV transition to the 4^+_1 state. In addition, a 1089-keV transition (doubly placed) was proposed to populate the 2150-keV level. An alternative placement for the 1089-keV transition is discussed in relation to a 2406-keV level below. The present data find a 831.1-keV transition strongly coincident with 1432-keV and 977-keV transitions, as shown in Fig. 8. Both of these transitions depopulate a previously identified level at 2294 keV (discussed below) and thus the 831-keV transition is given a new placement as directly populating the level at 2294 keV. A strong 830-keV transition is also observed in the γ-γ matrix, but is found to originate from ^{71}As [17], produced in a competing reaction channel. No evidence is found in the singles spectrum for a 2151-keV transition. Furthermore, gating on the 775-keV, $4^+_1 \rightarrow 2^+_1$ transition gives no indication of a 512-keV transition. With no support for any of the depopulating or populating transitions, the present data find no evidence for a level at 2150 keV.

A (2) level at 2294 keV was previously identified in (HI,xn) reactions [13] and observed to decay to the 2^+_1 and 2^+_2 states. In the present work, this level is observed and the two depopulating transitions confirmed. An additional 657-keV transition to the 4^+_1 state is also identified. This new transition is consistent with the prior (2) spin assignment. The statistics in the angle matrices were not sufficient to extract any further information on the spin of this level.

A level at 2372 keV was reported [13] to decay via four depopulating transitions to the 0^+_1, 2^+_1, 0^+_2, and 2^+_2 levels. These transitions were confirmed and found to have

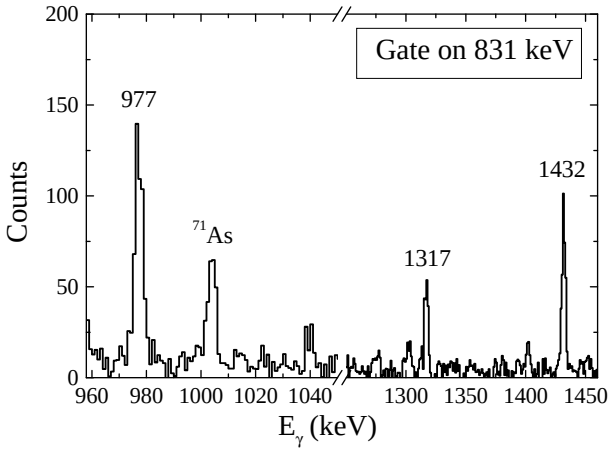

FIG. 8: Spectrum obtained by gating on the 831-keV transition providing evidence for its new placement as a transition feeding the level at 2294 keV.

intensity branches consistent with the literature values. Three new depopulating transitions to the 4_1^+, 0_3^+, and 2_3^+ states were observed in the present work (see Table I). The angular correlation analysis for the two strong depopulating transitions (1055 keV and 1510 keV) is given in Fig. 9. Both transitions point to a spin 2^+ assignment for this level, which is also consistent with all the observed decay branches. The 1055-keV transition is found to be mainly $E2$ in character, with a measured δ of $+7^{+19}_{-4}$, as shown in Fig. 9(a). The 1510-keV transition is found to have mainly $M1$ character with δ = -0.02(20), as shown in Fig. 9(b).

A level at 2406 keV was previously observed in (HI,xn) and (p,t) reactions [13] and assigned a spin of 3^-. In the (HI,xn) studies, a single transition of 1089 keV to the 2_2^+ state was observed. In the present work, a strong 1089-keV transition is observed in coincidence with the 380-keV, 454-keV, and 1317-keV transitions, all of which depopulate the 2_2^+ level, as shown in Fig. 4(a). Thus, the 1089-keV transition is associated with the decay of the 3^-, 2406-keV level observed in the (HI,xn) reactions. In the prior decay study [8], a 1089-keV transition was doubly placed as populating the 1876-keV and 2150-keV levels. As seen in Fig. 4(a), the 1089-keV transition is non-coincident with either of the strong transitions depopulating these levels (559 keV and 832 keV). Angular correlation analysis of the 1089-1317 keV cascade is consistent with a spin of 3 for the level and gives δ=-0.10(17), consistent with $E1$ multipolarity and therefore negative parity.

A level at 2434 keV was reported [13] to decay to the 2_2^+, 2_1^+, and 0_1^+ states through transitions of 1117 keV, 1572 keV, and 2434 keV, respectively and assigned a spin of 3^-. In the present work, no evidence is found for the 2434 keV transition to the ground state. Angular correlation analysis of the 1572-862 keV cascade is given in Fig. 9(c). A fit with a 3-2-0 cascade and δ=0 (assuming $E1$ multipolarity for the 1572-keV transition) is not

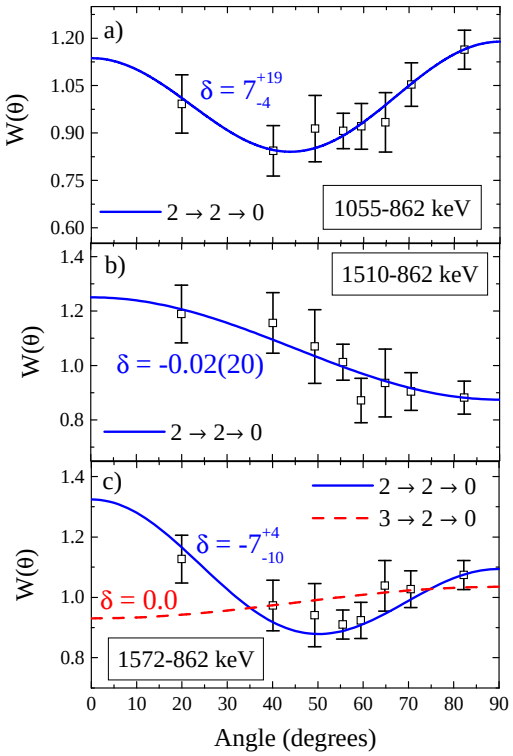

FIG. 9: Angular correlation analysis for the (a) 1055-keV, (b) 1510-keV, and (c) 1572-keV transitions. Data are indicated by the symbols, theoretical fits by the solid lines. The theoretical fits are calculated using the indicated δ values.

consistent with the data. The best fit is obtained with a spin 2 for the 2434-keV level and $\delta = -7^{+4}_{-10}$ for the 1572-keV transition.

Many additional changes were made to the previous level scheme of ^{72}Se. These are summarized in Table I. The present data find no support for the 2965-keV, 3226-keV, and 3240-keV levels proposed [8] in the prior β-decay study. The reported depopulating transitions from these levels were either given alternate placements in the level scheme or found to belong to contaminent nuclei. Many additional new levels were observed above 2.8 MeV. These are usually supported by two or more depopulating transitions.

Several of the newly identified levels are rather strongly populated in β decay. The parent ^{72}Br decaying states have different structures, the 1^+ ground state composed of particles in the fp shell [18] and the 3^- isomer involving occupancy in the $g_{9/2}$ orbit, and thus the strength distribution could provide some insight into the structure of states populated in ^{72}Se. The current experiment was not optimized for measuring the true β-decay strength distribution. The thick target, low-energy arrangement was very clean for γ-γ coincidence studies, but the spectra were not of sufficient quality to identify direct ground state decays from levels above 4 MeV in singles mode. Further, both ^{72}Br decays were involved and the contributions could not be separated in this data

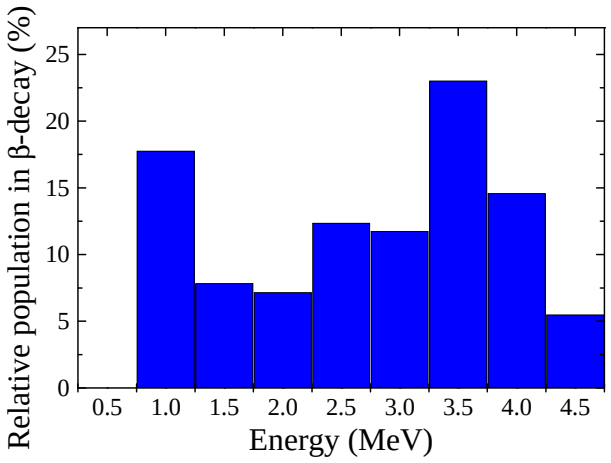

FIG. 10: (Color online) Relative population of states in ^{72}Se following the β-decay from ^{72}Br.

set. Despite these shortcomings, some information can be inferred about the β-strength distribution by determining the difference in γ flux populating and depopulating each level. This is illustrated in Fig. 10 which shows distinct peaks of population at the first excited state (which causes the high intensity in the 500-1000 keV bin) and to levels around 3.3 MeV. The former peak can be attributed to missing strength from high energy, low-intensity transitions populating the first excited state. However, the latter strength, arising from intense population of levels near 3.3 MeV appears to have a structural origin. It lies close to the quasi-particle excitation energy of states based on the deformed ^{72}Se configuration. Configurations of this type would be expected to be populated in the decay of the isomeric (10.3 sec) level in ^{72}Br as this parent level has proton occupancy of the $g_{9/2}$ shell-model state, the driver of deformed configuration. However, the overlap of parent and daughter states is far from complete; even if all the isomeric level decayed to this region the integrated strength would only have a logft value of 4.2(2). Nonetheless, in the future it would be interesting to confirm the isomer decays favor population of the $\sim$ 3.3 MeV excitation energy regime by performing a time resolved measurement to separate ground state and isomeric decays.

III. DISCUSSION

Several prior studies [6, 7, 12] have analyzed ^{72}Se in terms of simple two-level mixing of the 2^+ states and assuming 50%-50% admixtures. With the new branching ratios measured in the present work and new measurements of the lifetimes in the yrast band [4], we reinvestigate the applicability of simple two-level mixing. From the plot of moment of inertia (Fig. 1) it is clear that the mixing mainly occurs for low spin states. We expand upon the prior mixing studies and allow for mixing of both the 2^+ and 4^+ states, following the formalism outlined by Dickmann and Dietrich [19]. The 2^+ and 4^+ states are assumed to have mixed character, with a wavefunction of the form

$$|J_1\rangle = a_J|\varphi_J^{vib}\rangle + b_J|\varphi_J^{rot}\rangle. \quad (1)$$

In the simplest model, the 0_1^+ and 0_2^+ states are taken as purely vibrational and rotational in character, respectively, and the 6_1^+ state is taken as purely rotational. The solution of the Schrödinger equation for the mixed states is given by

$$E_{I\pm} = \frac{\varepsilon_I^{vib} + \varepsilon_I^{rot}}{2} \pm \frac{1}{2}\sqrt{(\varepsilon_I^{vib} - \varepsilon_I^{rot})^2 + 4h_I^2} \quad (2)$$

where E_I are the perturbed energies, ε the unperturbed energies, and h_I are the mixing matrix elements. For the vibrational states, the unperturbed energies are taken to follow a phonon scheme, with $\varepsilon^{vib} = (J/2)\hbar\omega$. The rotational states are described by a simple rotational energy formula with $\varepsilon^{rot} = \eta + \frac{J(J+1)\hbar^2}{2\mathcal{J}}$, where η is the bandhead energy and $\mathcal{J}$ is the moment of inertia of the band.

The a_J,b_J coefficients can be determined from the energies or $B(E2)$ transition strengths. As the latter are more sensitive to the wavefunctions, we use the yrast band $B(E2)$ strengths to deduce the mixing coefficients. Assuming that there is no overlap between the vibrational and rotational wavefunctions, the $B(E2)$ strengths can be written as [19]

$$\begin{aligned} B(E2)_{2\to0} &= a_2^2 B(E2)^{vib}_{2\to0} \\ B(E2)_{6\to4} &= b_4^2 B(E2)^{rot}_{6\to4} \\ B(E2)_{4\to2} &= a_2^2 a_4^2 2B(E2)^{vib}_{2\to0} + b_2^2 b_4^2 B(E2)^{rot}_{4\to2} \\ &+ a_2 b_2 a_4 b_4 \sqrt{2B(E2)^{vib}_{2\to0} B(E2)^{rot}_{4\to2}}. \end{aligned} \quad (3)$$

where the left-hand side of Eq. (3) corresponds to the measured $B(E2)$ values in the yrast band. To determine the pure rotational $B(E2)$ values included in the right-hand side of Eq. (3), it is assumed that the yrast band with $J^\pi \geq 8^+$ represents the pure deformed configuration. The intrinsic quadrupole moment, Q_o, of the rotational band was determined from the experimental $B(E2)$ values for the ground state band for $J^\pi \geq 8^+$. From the average, $Q_o = 2.16\ eb$, the pure rotational $B(E2)$ values for the lower spin states were deduced. The vibrational $B(E2)_{2\to0}$ strength is taken as a free parameter. The five unknowns, a_J,b_J, and $B(E2)^{vib}_{2\to0}$, are then determined using Eq. (3) along with the normalization conditions for a_J and b_J. We obtain, $a_2^2 = 0.55$, $b_2^2 = 0.45$, $a_4^2 = 0.17$, $b_4^2 = 0.83$ and $B(E2)^{vib}_{2\to0} = 41$ W.u. As expected, the first 2^+ states are nearly complete admixtures of vibrational and rotational wavefunctions. The 4_1^+ state, on the other hand, is mainly rotational in character.

TABLE II: $B(E2)$ transition strengths (in W.u.) in ^{72}Se compared with two-band mixing analysis (MIX) and the results of IBM-1 with configuration mixing (IBM-CM) calculations.

Transition	Exp	MIX	IBM-CM
$2_1^+ \rightarrow 0_1^+$	22.9(16)	22.9	25
$2_2^+ \rightarrow 0_1^+$	0.48(3)	18	1.6
$2_2^+ \rightarrow 0_2^+$	36(3)	29	33
$2_2^+ \rightarrow 2_1^+$	75(5)	18	45
$0_2^+ \rightarrow 2_1^+$	159(20)	116	53

In Table II, the experimental transition strengths from the 2_2^+ and 0_2^+ states are compared with the results of the band-mixing analysis using the a_2 and b_2 values extracted above. The large strengths of the $2_2^+ \rightarrow 0_2^+$ and $0_2^+ \rightarrow 2_1^+$ transitions are nicely reproduced by this simple model. The largest discrepancy is in the $2_2^+ \rightarrow 0_1^+$ transition which is significantly overpredicted. As discussed in Ref. [12], the strength of the $2_2^+ \rightarrow 0_1^+$ transition can be reduced by including a small amount of mixing into the 0^+ states in order to introduce some destructive interference.

Combining the extracted a_J and b_J values with the energy spacings in the yrast band, the mixing matix elements and the unperturbed energies can be determined. We obtain for the mixing matrix elements, h_2 = -237 keV and h_4 = -205 keV. The unperturbed energy of the 2_1^+ state is determined to be ε = 1.102 MeV, while the unperturbed 0_2^+ energy is determined to be η = 876 keV with the moment of the inertia given by $\hbar^2/2\theta$ = 37.4 keV. The moment of inertia obtained through the mixing analysis is consistent with what is deduced by fitting the yrast states with $J > 6^+$ with a simple rotational energy formula which gives $\hbar^2/2\mathcal{J}$ = 35.5 keV. The mixing matrix element for the 2^+ states is approximately half the energy separation of the final perturbed states, again indicating maximal mixing and nearly degenerate unperturbed energies.

In the above analysis, we used a model that assumed a spherical ground state for ^{72}Se. As several prior works have suggested an oblate ground state structure, we also explored that possibility. In Eq. (3), the structure of the ground state is incorporated by taking $B(E2)^{vib}_{4\rightarrow 2} = 2B(E2)^{vib}_{2\rightarrow 0}$, in the equation for $B(E2)_{4\rightarrow 2}$. We can instead assume an oblate structure by taking the relation, $B(E2)^{vib}_{4\rightarrow 2} = \frac{10}{7}\, B(E2)^{vib}_{2\rightarrow 0}$. The mixing coefficients then become a_2^2 = 0.496, b_2^2 = 0.504, a_4^2 = 0.17, b_4^2 = 0.83 and $B(E2)^{vib}_{2\rightarrow 0}$ = 46 W.u. These results are not significantly different from the calculations assuming a vibrational ground state, and change the extracted $B(E2)$ strengths and unperturbed energies by only a few percent.

Clearly, simple two-level mixing does not differentiate between a spherical or oblate ground state structure in ^{72}Se. Instead, we turn to a more flexible model, the interacting boson model (IBM) [20]. The Se isotopes have been described by IBM-2 calculations, where a distinction is made between protons and neutrons. In these studies [21, 22], it was found that the isotopes with $N \geq 40$ could be well described, whereas significant discrepancies were found for the $N < 40$ isotopes, particularly in the energy of the 0_2^+ state. To incorporate the presence of shape coexistence, we performed IBM with configuration mixing [23, 24] calculations (IBM-CM). Using the IBM-1 formalism where there is no distinction between protons and neutrons, the system is composed of regular states with the standard N bosons which mix with deformed states corresponding to N+2 bosons. The latter arises from the assumption that the deformed configuration consists of two particles being promoted into a higher lying shell or orbit. For ^{72}Se, this corresponds to $N_{reg} = 8$ and $N_{def} = 10$ with the deformed configuration based on particles in the $g_{9/2}$ orbit. The full Hamiltonian is given by [23, 24] $\hat{H} = \hat{H}_{reg}\hat{P}_{reg} + \hat{H}_{def}\hat{P}_{def} + \hat{V}_{mix}$ where $\hat{P}$ are projection operators and where

$$\begin{aligned} \hat{H}_{reg} &= \epsilon_{reg}\hat{n} + \kappa_{reg}\hat{Q}_{reg}\hat{Q}_{reg} \\ \hat{H}_{def} &= \epsilon_{def}\hat{n} + \kappa_{def}\hat{Q}_{def}\hat{Q}_{def} + \Delta \\ \hat{V} &= \alpha_o(s^\dagger s^\dagger + ss)^{(0)} + \beta_o(d^\dagger d^\dagger + dd)^{(0)} \end{aligned} \quad (4)$$

with $\hat{Q}_{reg(def)} = (s^\dagger d + d^\dagger s)^{(2)} + \chi_{reg(def)}(d^\dagger d)^{(2)}$.

Each configuration has the parameters ϵ,κ,χ and e_b (where e_b is the effective boson charge for the $E2$ operator). The ratio of ϵ/κ sets the deformation of a given configuration. The parameter χ controls the degree of axial symmetry. It can range from -$\sqrt{7}/2$ to +$\sqrt{7}/2$ with the limits χ = -$\sqrt{7}/2$ for axially symmetric prolate, $\chi = 0$ for γ-soft, and χ = +$\sqrt{7}/2$ for axially symmetric oblate. The α_o, β_o parameters control the strength of the mixing and the parameter Δ is approximately the single-particle energy required to promote a pair of particles.

Usually in IBM configuration mixing calculations, the ϵ,κ,χ and e_b parameters are determined by fitting nearby isotopes where either the spherical or deformed configuration is thought to dominant. As this is a region with rapidly changing shapes, it is difficult to find neighboring isotopes which correspond to the pure configurations. Instead, we make use of the results of the two-band mixing calculations to determine the parameters for the two configurations. We obtain ϵ_{reg} = 1.25, ϵ_{def} = 0.83, κ_{reg} = -0.02 κ_{def} = -0.03, χ_{reg} = 1.32, χ_{def} = -1.00, $e_{b(reg)}$ = 1.55, $e_{b(def)}$ = 1.35.

The mixing terms, α_o, β_o, and the gap, Δ, are then taken as free parameters and adjusted to reproduce both the energies and $B(E2)$ transition strengths. The best fit is obtained with $\alpha_o = \beta_o$ = 0.045 and Δ = 1.21 MeV.

The results of the IBM-CM calculations for ^{72}Se are given in Figure 11. Some absolute $B(E2)$ transition strengths are also included in Table II for comparison. Overall, good agreement is obtained for both energies and $B(E2)$ strengths. The configuration of the states in terms of the percentage of the regular (N) and deformed (N+2) configurations is consistent with previous

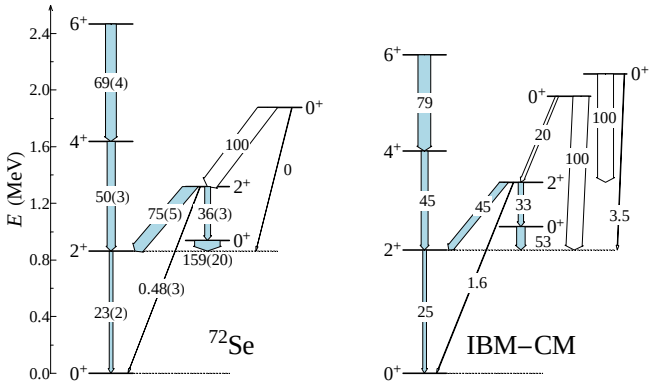

FIG. 11: (Color online) Level scheme for ^{72}Se compared with calculation using the IBM with configuration mixing (IBM-CM). The shaded transitions are labeled by their absolute $B(E2)$ strength (in W.u.) while white arrows indicate relative transition strengths normalized to the strongest branch.

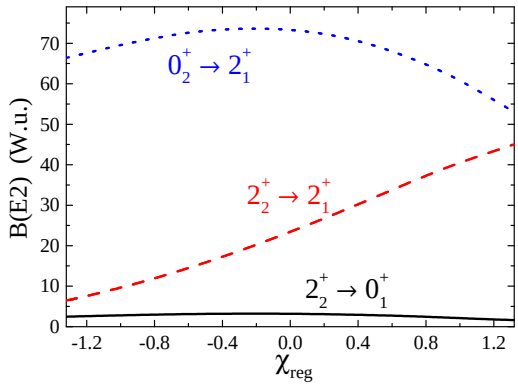

FIG. 12: (Color online) $B(E2)$ strengths for ^{72}Se from the IBM-CM calculations. The best fit parameters (see text) are kept constant except for the parameter χ_{reg} which is allowed to vary from axially symmetric prolate ($\chi = -\sqrt{7}/2$) to γ-soft ($\chi = 0$) to axially symmetric oblate ($\chi = +\sqrt{7}/2$).

interpretations of ^{72}Se. The ground state wavefunction is composed of 88% the regular configuration while the 0^+_2 state wavefunction is composed of 88% of the deformed configuration. The first two excited 2^+ states are strong admixtures of both configurations, with the 2^+_1 having 40% of the N configuration and 60% of the N +2 configuration. The 4^+_1 state wavefunction exhibits 85% of the deformed configuration.

An interesting feature of these calculations is in the strength of the $B(E2;\ 2^+_2 \rightarrow 2^+_1)$ transition. In the two level mixing calculations, even with maximal mixing between the 2^+ states, the predicted value (18 W.u.) is quite a lot smaller than the experimental value (75(5) W.u.). In the IBM-CM calculations, this transition is highly sensitive to the value of χ used for the normal configuration. Keeping all of the parameters constant and varying only χ_{reg}, the energy spectrum and most $B(E2)$ transition strengths change only slightly (on the order of ∼10%) while the $B(E2;\ 2^+_2 \rightarrow 2^+_1)$ transition strength changes rather substantially, as shown in Fig. 12. The $B(E2;\ 2^+_2 \rightarrow 2^+_1)$ strength is a maximum for an axial oblate structure ($\chi = +\sqrt{7}/2$) and decreases rapidly for smaller values of χ. This supports the suggestion of the lowest states in ^{72}Se having an oblate shape and is consistent with recent microscopic calculations.

The states discussed thus far involve only the yrast levels of the two configurations. In principle, each of the different shapes should also have so-called "β" and "γ" collective vibrations built upon them. An interesting feature of the IBM calculations is the prediction of two closely spaced 0^+ states lying near 2 MeV. These 0^+ states are predicted to be completely mixed and arise from states built on the ground state and prolate configurations. In the absence of any mixing, it would be expected that one 0^+ state decays predominantly to the ground state and the other to the prolate configuration. This decay pattern is observed in the calculations (Fig. 11) despite the fact that both the $0^+_{3,4}$ and $2^+_{1,2}$ states are strongly mixed. Based on the observed decay properties, the new 0^+ state observed at 1876 keV can be identified with the 0^+_4 state in the IBA calculations and thus would correspond to a collective vibration in the deformed minima.

In conclusion, the low-lying excited states in ^{72}Se have been investigated following the β decay of ^{72}Br. The decay scheme was extended and revised based on high quality γ-γ coincidence data and angular correlations were measured. Evidence is found for population of two different configurations; one set of levels based on the groundstate which are probably slightly oblate-deformed but soft to vibrations, and another based on a state with considerable prolate deformation. Two-level mixing places the unperturbed excited band at ∼ 875 keV. However, the interaction between configurations is very large, ∼ 225 keV, and the mixing between the lowest J = 2 states is almost complete. The strong mixing suggests that the barrier between the configurations is not sufficiently high or thick to localize the wavefunctions in their respective minima. Consequently, the intuitive classical concept of well-defined "shapes" is lost for the lowest levels, although probably more appropriate at higher spins. This is consistent with beyond-mean-field Hartree Fock calculations for this region. The β-decay strength is found to be peaked in a few states near 3.3 MeV, possibly due to particle-hole excitations based on the deformed configuration.

IV. ACKNOWLEDGMENTS

This work was supported by U.S. DOE Grant No. DE-FG02-91ER-40609 and by the DOE Office of Nuclear Physics under contract DE-AC02-06CH11357.

[1] S.M. Fischer, D.P. Balamuth, P.A. Hausladen, C.J. Lister, M.P. Carpenter, D. Seweryniak, and J. Schwartz, Phys. Rev. Lett. **84**, 4064 (2000).

[2] J. Heese, K.P. Lieb, L. Lühmann, F. Raether, B. Wörmann, D. Alber, H. Grawe, J. Eberth, and T. Mylaeus, Z. Phys. A **325**, 45 (1986).

[3] A.M. Hurst *et al.,* Phys. Rev. Lett. **98**, 072501 (2007).

[4] J. Ljungvall *et al.,* Phys. Rev. Lett. **100**, 102502 (2008).

[5] A Obertelli *et al.,* Phys. Rev. C **80**, 031304(R) (2009).

[6] J.H. Hamilton, A.V. Ramayya, W.T. Pinkston, R.M. Ronningen, G. Garcia-Bermudez, H.K. Carter, R.L. Robinson, H.J. Kim, and R.O. Sayer, Phys. Rev. Lett. **32**, 239 (1974).

[7] A.V. Ramayya, R.M. Ronningen, J.H. Hamilton, W.T. Pinkston, G. Garcia-Bermudez, R.L. Robinson, H.J. Kim, H.K. Carter, and W.E. Collins, Phys. Rev. C **12**, 1360 (1975).

[8] W.E. Collins, J.H. Hamilton, R.L. Robinson, H.J. Kim, J.L.C. Ford, Jr., Phys. Rev. C **9**, 1457 (1974).

[9] Nobuo Hinohara, Takashi Nakatsukasa, Masayuki Matsuo, and Kenichi Matsuyanagi, Phys. Rev. C **80**, 014305 (2009).

[10] A. Petrovici, K.W. Schmid, and A. Faessler, Nucl. Phys. A **710**, 246 (2002); **728**, 396 (2003).

[11] K. Kaneko, M. Hasegawa, and T. Mizusaki, Phys. Rev. C **70**, 051301(R) (2004).

[12] K.P. Lieb and J.J. Kolata, Phys. Rev. C **15**, 939 (1977).

[13] D. Abriola and A.A. Sonzogni, Nucl. Data Sheets **111**, 1 (2010).

[14] CSCAN sorting package, `http://wnsl.physics.yale.edu/cscan`

[15] D.C. Radford, Nucl. Instrum. Methods Phys. Res., Sect. A **361**, 297 (1995).

[16] James E. Draper, Nicholas S.P. King, and Walter G. Wyckoff, Phys. Rev. C **9**, 948 (1974).

[17] M.R. Bhat, Nucl. Data Sheets **68**, 579 (1993).

[18] I. Piqueras *et al.,* Eur. Phys. J. A **16**, 313 (2003).

[19] F. Dickmann and K. Dietrich, Z. Phys. A **271**, 417 (1974).

[20] F. Iachello and A. Arima, *The Interacting Boson Model* (Cambridge University Press, Cambridge, 1987).

[21] F.S. Radhi and N.M. Stewart, Z. Phys. A **356** 145 (1996).

[22] U. Kaup, C. Monkemeyer, and P.V. Brentano, Z. Phys. A **310**, 129 (1983).

[23] P.D. Duval and B.R. Barrett, Phys. Lett B **100**, 223 (1981).

[24] P.D. Duval and B.R. Barrett, Nucl. Phys. A **376**, 213 (1982).